

AB Doradus C: Age, Spectral Type, Orbit, and Comparison to Evolutionary Models

E.L. NIELSEN^{1,*}, L.M. CLOSE¹, J.C. GUIRADO², B.A. BILLER¹, R. LENZEN³, W. BRANDNER³, M. HARTUNG⁴, and C. LIDMAN⁴

¹ Steward Observatory, University of Arizona, 933 N. Cherry Ave, Tucson, AZ 85721 USA

² Departament d'Astronomia i Astrofísica, Universitat de València, E-46100 Burjassot, Valencia, Spain

³ Max-Planck-Institut für Astronomie, Königstuhl 17, D-69117 Heidelberg, Germany

⁴ European Southern Observatory, Alonso de Cordova 3107, Santiago 19, Chile

Received <date>; accepted <date>; published online <date>

Abstract. We expand upon the results of Close et al. 2005 regarding the young, low-mass object AB Dor C and its role as a calibration point for theoretical tracks. We present an improved spectral reduction and a new orbital solution with two additional epochs. Our improved analysis confirms our spectral type of M8 (± 1) and mass of $0.090 \pm 0.003 M_{\odot}$ for AB Dor C. Comparing the results for AB Dor C with other young, low-mass objects with dynamical masses we find a general trend where current evolutionary models tend to over-predict the temperature (or under-predict the mass) for low mass stars and brown dwarfs. Given our precision, there is a $\sim 99\%$ chance that the mass of AB Dor C is underestimated by the DUSTY tracks in the HR diagram.

Key words: Infrared: Stars, Stars: Formation, Stars: Low-Mass, Brown Dwarfs, Stars: Pre-Main-Sequence, Stars: Individual: AB Dor

©0000 WILEY-VCH Verlag GmbH & Co. KGaA, Weinheim

1. Introduction

The study of young, low-mass objects has been yielding increasingly fruitful science, yet the field remains dependent on evolutionary models to properly interpret the data that are collected from these objects. In particular, mass, while a fundamental property, is very rarely measured directly, and instead must be inferred from theoretical tracks (e.g., Burrows, Sudarsky, and Lunine 2003, Chabrier et al. 2000). It is thus of great interest to find calibrating objects that can link a dynamically measured mass with observables such as NIR (1–2 μm) fluxes and spectral types.

In our previous work (Close et al. 2005), we reported the direct detection of the low-mass companion to the young star AB Dor A, along with measurements of the JHKs fluxes, spectral type, and dynamically determined mass of AB Dor C. Upon comparing these results with the predictions of Chabrier et al. 2000, we found the models to be systematically over-predicting the fluxes and temperature of AB Dor

C, given an age of the system of 50 Myr. Put another way, the model masses seem to be underestimating the mass of a low-mass object given its age, NIR fluxes, and spectral type. Since the publication of these results, another calibrating object has been reported by Reiners, Basri, and Mohanty 2005: USco CTIO 5. While this equal-mass binary is younger (~ 8 Myr) and more massive (total mass $\geq 0.64 M_{\odot}$) than AB Dor C, Reiners et al. find the same trend of models under-predicting masses based simply on photometric and spectroscopic data applied to the HR diagram. A similar trend for such masses was previously noted by Hillenbrand and White 2004. Moreover, this trend has been theoretically predicted for higher masses by Mohanty, Jayawardhana, and Basri 2004, and by Marley et al. 2005 for planetary masses.

In this paper, we seek to expand on our earlier results from Close et al. 2005, using an improved spectral reduction and a more robust determination of the spectral type. We also present an improved orbital fit based on additional astrometric data, as well as address concerns raised by Luhman, Stauffer, and Mamajek 2005 regarding the age of the AB Dor system.

Correspondence to: enielsen@as.arizona.edu

* E. Nielsen acknowledges the support of the Michelson Science Center Graduate Student Fellowship.

2. An Improved Spectral Reduction

As described in Close et al. 2005, in February 2004 we obtained 20 minutes of K-band spectra using the Very Large Telescope (VLT), following our initial detection of AB Dor C. Using the $R \approx 1200$ -1500 (2 - $2.5 \mu\text{m}$) grism and the $0.027''$ pixel camera of NACO (see Lenzen et al. 2003), the $0.086''$ slit was aligned along the centers of both AB Dor A and C. The observations themselves consisted of eight deep exposures, intentionally saturating the inner pixels of the spectral PSF, with the two objects (A and C) nodded along the slit between exposures. An additional eight exposures were obtained with a 180° rotation of the derotator, flipping the relative positions of A and C.

Given our measured separation of A and C of $0.156''$ (5.78 pixels), and a flux ratio at Ks of 80, the signal from AB Dor C lies beneath the wings of the PSF of A. Relying on the relative stability of the NACO PSF, we subtracted a 0° image from a 180° , removing the signal from A while leaving a positive and negative spectrum of AB Dor C, which can then be extracted easily using the standard Image Reduction and Analysis Facility (IRAF) routines. This aligning of the PSFs is complicated by sub-pixel variations in the order position and orientation from image to image, as well as by variations in the total flux across different exposures.

To prepare for this subtraction, the first step is to align the 0° and 180° images. This pair of images is considered one dispersion pixel at a time (that is, we consider the 1024 spatial pixels along the chip corresponding to a single wavelength element), where one image undergoes a series of sub-pixel shifts before the two one-dimensional segments are subtracted. A series of reference pixels between 9 and 12 pixels ($0.24''$ and $0.32''$) from the center of the PSF are chosen so as to avoid the saturated central pixels, and any signal from AB Dor C (which would be asymmetric from 0° to 180°). The minimum variance in these reference pixels after subtraction is taken to correspond to the best shift. This process is repeated for each of the 1024 dispersion pixels, a polynomial is fit to these individual shifts, and this fit is used to prepare the final subtraction.

We continue this procedure iteratively with various values of a global flux scaling of one of the two images, again minimizing the variance in the reference pixels to find the best fit. An example of this subtraction of a 0° and 180° image is shown in Figure 1. Each point represents a sum across all 1024 dispersion pixels corresponding to a given spatial pixel, with the dashed lines indicating the location of AB Dor C. The inner, saturated pixels show a large amount of noise as would be expected, but at the position of AB Dor C are obvious negative and positive peaks. We repeat these steps for each possible pairing of the eight 0° and eight 180° spectra, eliminating pairs where the routine did not converge, and choosing the best subtraction; this yields a total of 13 spectra (out of 16 possible), which are then combined.

We note that while there are many pairs where this process fails to converge, we never see a “false-positive” signal. That is, while for many of our spectra we see a positive peak to the right and a negative peak to the left, as seen in Fig-

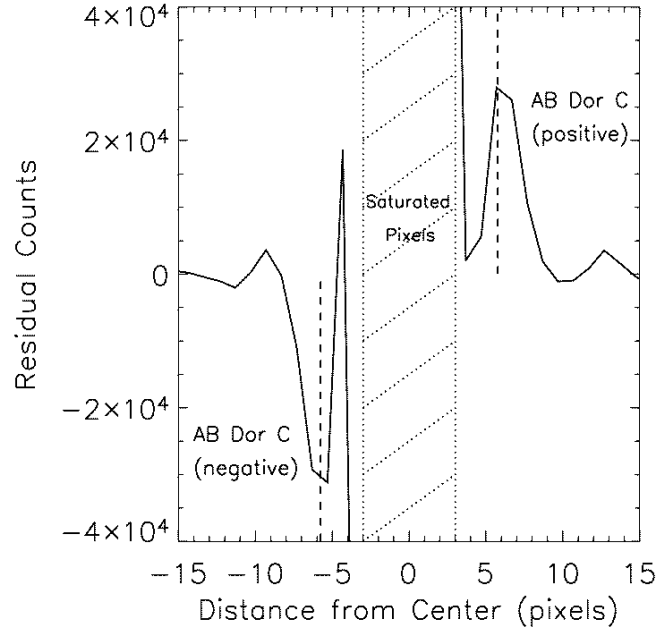


Fig. 1. An example of a subtraction of a 0° image from a 180° , with each spatial pixel along the x-axis representing a sum along the dispersion direction. The expected positions of AB Dor C on either side are marked with dashed lines; the clear positive and negative signals at this location indicate a good subtraction of AB Dor A. The spectrum is extracted from both the positive peak on the right, as well as the negative peak on the left. The marked central region (where the data are not plotted) indicate the saturated pixels which were ignored during the reduction.

ure 1, not even once (out of 64 trials) do we see a positive peak on the left or a negative peak on the right at the position of AB Dor A. This leaves us confident that we have extracted the signal from AB Dor C, rather than spurious light. Additionally, these 13 independent extractions of the spectra are all qualitatively similar; each appears as a late-M spectrum, clearly distinguishable from the spectrum of AB Dor A.

Observations of a standard star (HIP 24153, G3V) taken within a half hour of the AB Dor images are used to remove telluric lines, and a modified solar spectrum compensates for stellar features from the standard (Maiolino, Rieke & Rieke 1996).

The final spectrum is shown plotted against two young, late-M templates in Figures 2 and 3. Since we were unable to preserve the continuum of AB Dor C through our data reduction, we simply remove the continuum from our spectrum as well as that of the template (using polynomial fits of the same order). Judging by the depth of the CO breaks, and the strength of the Na I line at $2.21 \mu\text{m}$, these templates constrain the spectral type of AB Dor C between M7 and M9.5 at the 1σ level, as was previously reported in Close et al. 2005. Additionally, we found four features in the spectrum that do not seem consistent with any late-M. We compared our unsaturated spectrum of AB Dor A to other K1 spectra, and finding these features present in A as well, we determined these lines

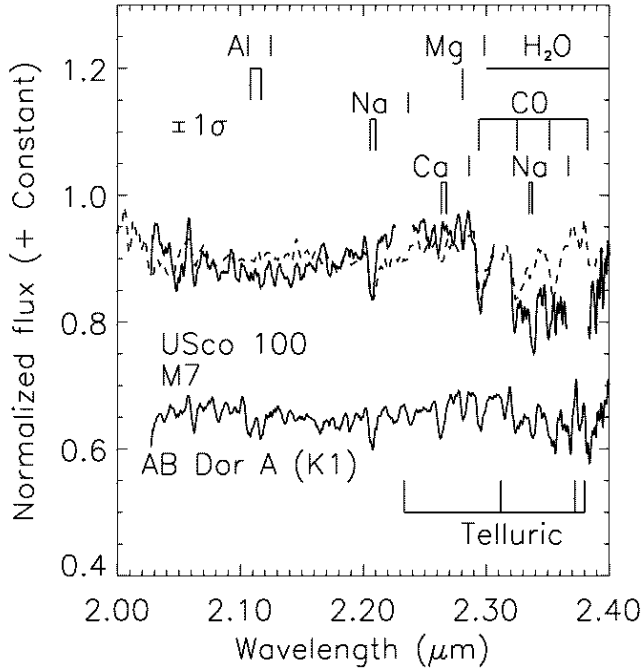


Fig. 2. The spectrum of AB Dor C (upper solid line) shown against that of USco 100 (dashed line), a young (~ 8 Myr) M7 (Gorlova et al. 2003), with the continuum of both objects removed. Features arising from an incomplete removal of telluric lines are marked, and are not plotted in the AB Dor C spectrum. The strength of C’s sodium line at $2.21 \mu\text{m}$ and the depth of the H_2O absorption and the first CO break at $2.3 \mu\text{m}$ suggest AB Dor C is cooler than an M7, at the 1σ level of the observational noise, as indicated in the figure (this noise, 0.015, was found by taking the standard deviation of the AB Dor C spectrum between 2.13 and $2.18 \mu\text{m}$, a featureless section of spectrum between the Al I and Na I doublets). The spectrum of AB Dor A (which was used as a reference for poorly-removed telluric features) is also shown at the bottom of the plot.

to be telluric features that were not fully removed, hence we have not plotted these small segments of the spectra.

We note in Figures 2 and 3 that while both AB Dor A and C show a Na I line at $2.21 \mu\text{m}$ and CO features between 2.3 and $2.4 \mu\text{m}$, AB Dor A shows a strong $2.26 \mu\text{m}$ Ca I triplet absorption feature while AB Dor C does not. Similarly, there is no correlation between the strength of the Mg I line ($2.28 \mu\text{m}$) or the Al I doublet ($2.11 \mu\text{m}$) between A and C, as would occur if our spectrum were dominated by spurious light from AB Dor A. Comparing the line strengths, we find the equivalent width of the Na I $2.21 \mu\text{m}$ doublet in C to be ~ 1.5 times that of A. Meanwhile, the Ca I $2.26 \mu\text{m}$ feature equivalent width for C is less than 5% of A. This leaves us confident that the amount of contamination from AB Dor A is $\leq 5\%$, with similar results obtained from analysis of the Al I doublet.

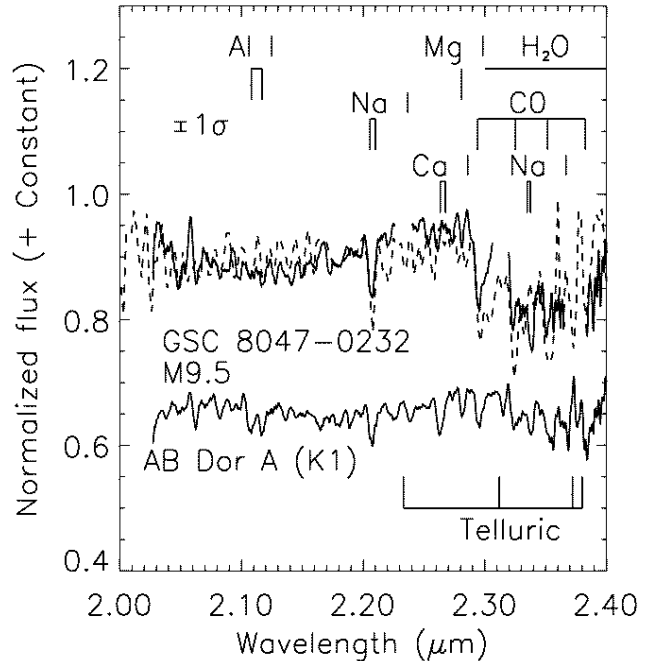


Fig. 3. The spectrum of AB Dor C, this time plotted with GSC 8047-0232, a young (~ 30 Myr) M9.5 (Chauvin et al. 2005). The sodium and CO features of the template now appear cooler than those of AB Dor C, bounding the spectral type between M7 and M9.5, at the 1σ level.

3. Improved Orbit

Our earlier paper (Close et al. 2005) was based on observations conducted at the VLT in February of 2004. Since this work was published, we have reduced additional Simultaneous Differential Imaging (SDI, see Lenzen et al. 2004) data from September and November of 2004. While data through the narrow-band SDI filters do not provide us with any improved photometric information (beyond confirmation that between AB Dor A and C, $\Delta H = 5.20$), these images do give us additional astrometric data points, allowing us to refine the orbit. Figure 4 shows each epoch of measuring the position of AB Dor C with respect to A.

We fit our three VLT SDI data points for the relative position between AB Dor A and C along with the existing VLBI/Hipparcos astrometry for AB Dor A (Guirado et al. 1997) to obtain an improved orbit of the reflex motion of AB Dor A. For this fit, we followed the procedure described in Guirado et al. 2005 (submitted). The new orbital elements are shown in Table 1, and are mostly similar to those published in Close et al. 2005. The two orbits are compared with respect to the three 2004 epochs of SDI observations in Figure 5.

The most immediate consequence of our new orbital fit is that the mass of AB Dor C remains at $0.090 M_{\odot}$. As reported in Guirado et al. 2005, we notice that the error bars shrink from $0.005 M_{\odot}$ to $0.003 M_{\odot}$. This confidence with which we know the mass of AB Dor C makes it an ideal object for calibrating theoretical evolutionary tracks.

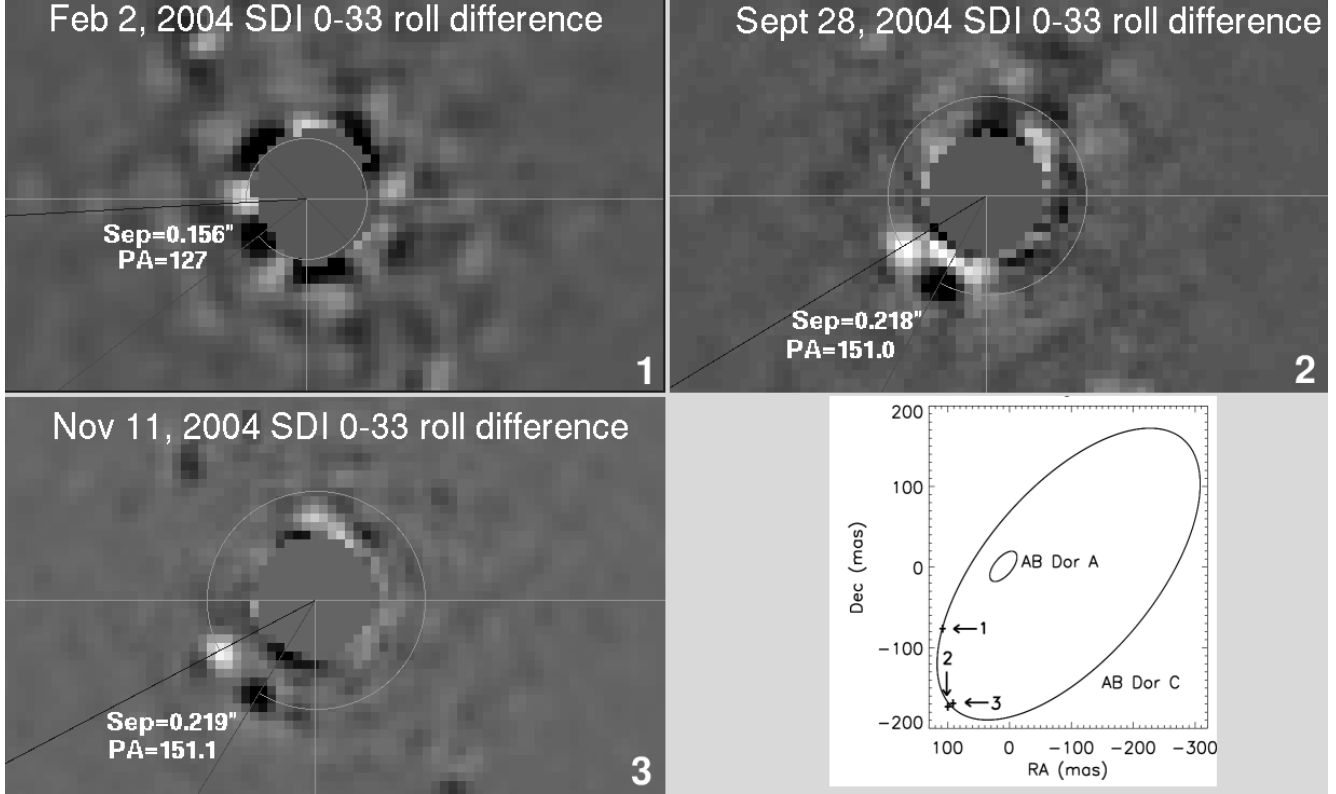


Fig. 4. The different epochs of AB Dor C measured during 2004 with the VLT SDI device. Each of the numbered panels shows an individual epoch of SDI observations, with images at position angles of 0° and 33° subtracted from each other, showing a positive and negative signal from AB Dor C. The inner pixels of AB Dor A have been intentionally saturated, and have been removed from the image. The orbital motion of the companion can clearly be seen over this span of time. The bottom-right panel shows these locations against a plot of the full orbit of AB Dor C. The 11 additional VLBI/Hipparchos measurements of the reflex motion of AB Dor A (which went into finding the orbital solution) are not shown on this plot (See Close et al. 2005).

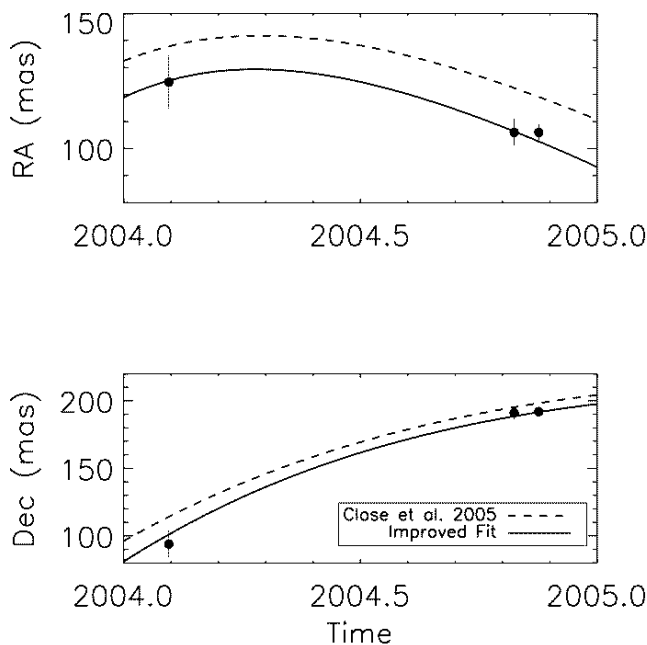


Fig. 5. Detail of the reflex orbit of AB Dor A for the time period of our SDI observations. The previous orbit (Close et al. 2005) is also shown.

Table 1. Our improved parameters for the reflex motion of AB Dor A.

Parameter	Value	Error	Units
Period	11.74	0.07	years
Semi-Major Axis	0.0319	0.0008	“
Semi-Major Axis	0.476	0.012	AU
Eccentricity	0.61	0.03	
Inclination	66	2	deg.
Argument of Periastron	110	3	deg.
Position Angle of Node	133	2	deg.
Epoch of Periastron Passage	1991.92	0.03	years
Mass of AB Dor C	0.090	0.003	M_\odot

4. Discussion

4.1. Spectral Type

Using our new spectrum, we attempt to refine the determination of the spectral type of AB Dor C. Rather than use field objects as our standards (as we did in Close et al. 2005), we choose young objects (with lower surface gravities) to constrain the spectral type. Figure 6 shows our AB Dor C spectrum plotted against a variety of young, late-M spectra (WL 14, USco 67, USco 66, and USco 100 from Gorlova et

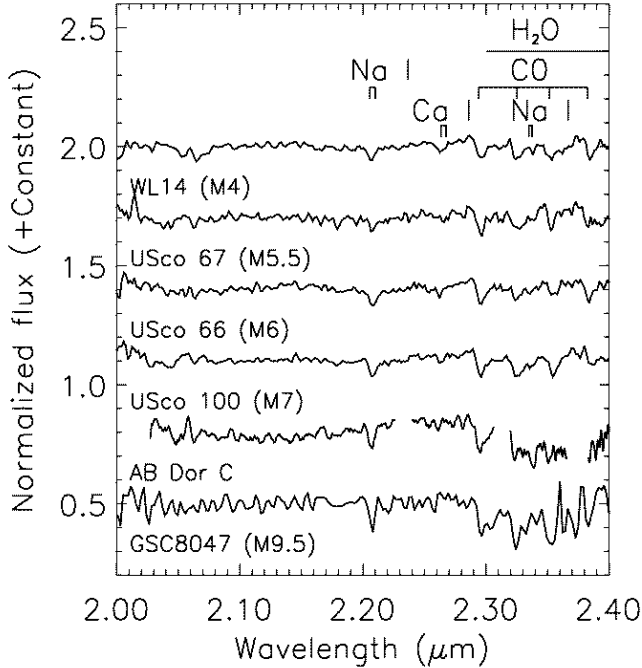


Fig. 6. The spectrum of AB Dor C shown against a number of young (~ 10 Myr), low-surface gravity objects. The features seem to be bound between the M7 and M9.5 templates.

al. 2003, GSC 8047-0232 from Chauvin et al. 2005). Again, since AB Dor C lacks a continuum, we have removed the continuum of all the objects (using the same order of polynomial fit) for comparison purposes. Trends across the sequence are clearly visible: as we move to later spectral types, the strengths of the Na line, CO breaks, and H₂O absorption increases, while the Ca line weakens. For all these features, AB Dor C seems best bound between the M9.5 and M7 templates at 1σ , agreeing with the J-Ks $\sim 1.3 \pm 0.4$ magnitude color reported in Close et al. 2005.

All of the templates used in Figure 6 are significantly younger than AB Dor C. To properly bound the spectral type, we consider field objects, as we did in Close et al. 2005. Figure 7 again shows AB Dor C, now with templates of higher surface gravity (spectra from Cushing, Rayner, and Vacca 2005; since these spectra were taken at higher resolution, we have smoothed them to match the resolution of AB Dor C). The spectra no longer fit as nicely (especially the shapes of the CO features), but as before, the spectrum seems to fit best in the sequence between an M7 and an M9.

4.2. The Age of AB Dor

In Close et al. 2005 it was argued that due to the excess luminosity of AB Dor A and C compared to the Pleiades, and A's large Li equivalent width and very fast rotation, that the age of the system was 30-100 Myr. An age of 50 ($-20, +50$) Myr was adopted, which was consistent with the 50 Myr published age of the AB Dor moving group (Zuckerman, Song, and Bessell 2004). Recently Luhman et al. 2005 has suggested a slightly older age of 70-150 Myr. However, as Luhman et al. 2005 notes, the AB Dor moving group is systematically

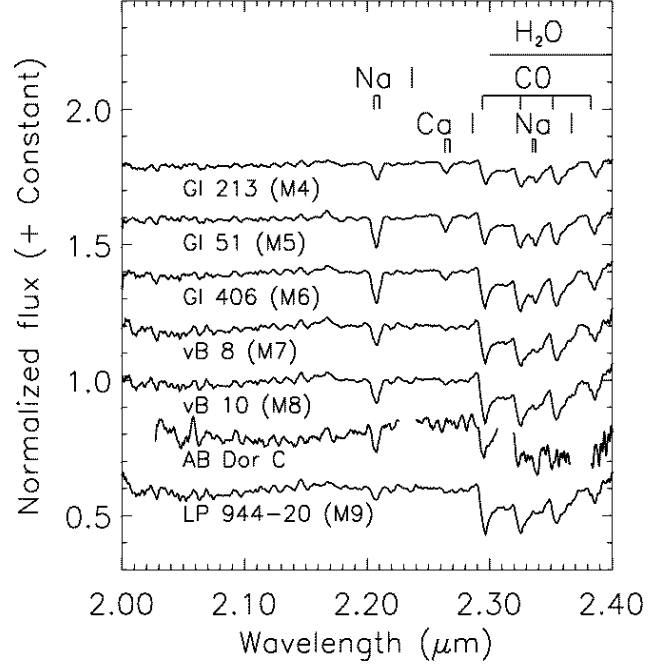


Fig. 7. The spectrum of AB Dor C, this time plotted against field M dwarfs (~ 5 Gyr), with higher surface gravities. Again, a spectral type of $M8 \pm 1$ (1σ) seems most consistent with our spectrum.

over-luminous compared to the Pleiades (age 100-120 Myr) by ~ 0.1 magnitudes in M_{Ks} vs. V-Ks plots (see their Figure 1).

We have found similar results with a near-infrared color magnitude diagram, as seen in Figure 8. While the two groups of stars appear similar for the early-type members (where the isochrones overlap), beyond a color of J-Ks ~ 0.4 , the lower main sequence of the AB Dor Moving group appears to be above that of the Pleiades by about 0.15 magnitudes. We have run a series of simulations that suggest that only $\sim 10\%$ of the time would a group of Pleiades aged stars appear 0.15 magnitudes above the single-star locus as is observed for all the AB Dor group members.

We note that a 0.15 magnitude offset from the Pleiades single star locus suggests a group age of ~ 70 Myr from the Lyon group's models (Baraffe et al. 1998). We adopt an average age of 70 ± 30 Myr with 1σ error bars. Hence, there is a $\sim 10\%$ chance that the AB Dor moving group is as old as the Pleiades based on these color-magnitude diagrams.

Luhman et al. 2005 concludes that their increase in the age of the system (from 50 to 120 Myr) implies that the luminosity is correctly predicted by the models. But, as we will see in Section 4.3, even if the luminosity is close to the predicted value at an age of 100 Myr and $0.09 M_{\odot}$, there is still a very large error in the temperature. Hence, the models will overestimate the temperature (or underestimate the mass) of young, low-mass objects in the HR diagram regardless of the 70 or 120 Myr age of AB Dor.

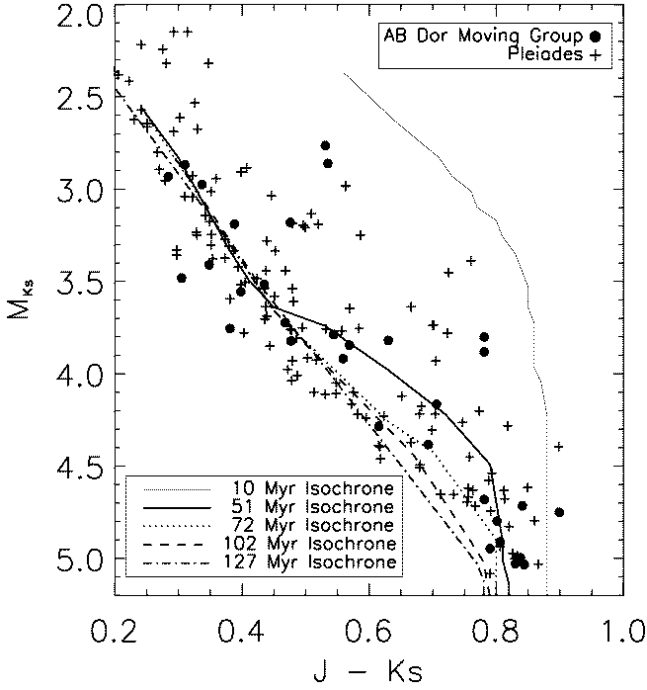


Fig. 8. A NIR color-magnitude diagram of medium-mass members of the Pleiades (compiled from the literature) and the AB Dor moving group (Zuckerman et al. 2004), with the theoretical isochrones of Baraffe et al. 1998. The offset between the single star locus of the two groups redward of $J-K_s \sim 0.4$ suggests a younger age for the AB Dor moving group, closer to 70 Myr.

4.3. HR Diagram and Evolutionary Models

In order to further compare our observations of AB Dor C with the theoretical models, we consider an HR diagram with our measured values and the DUSTY models. Using our spectral type of M8 and the absolute K_s from Close et al. 2005, we can derive an effective temperature and bolometric luminosity for AB Dor C. We plot AB Dor C in such an HR diagram in Figure 9, along with the DUSTY tracks, AB Dor Ba/Bb, and low-mass members of the Pleiades. We compile Pleiades members from Martin et al. 2000, as well as from other sources in the literature (Cluster identifications and spectral types from Briggs and Pye 2004, Pinfield et al. 2003, Terndrup et al. 1999, Festin 1998, Martin, Rebolo, and Zapatero-Osorio 1996, and K_s -band fluxes from the 2MASS catalog). The bolometric luminosities and temperatures for all these objects (AB Dor Ba/Bb, C, and the Pleiades members) are derived using Allen et al. 2003 and Luhman 1999 (dwarf scale), respectively.

As is seen in Figure 9, AB Dor C is overluminous, above the Pleiades sequence (as expected from a younger object, ~ 70 Myr). We also show an arrow to its position in the HR diagram predicted by the DUSTY models appropriate to its age and mass.

It has been suggested that this overluminosity could be explained if AB Dor C were a close, unresolved binary (Martin private communication; Marois et al. 2005). Were this the case, AB Dor C would split into two points in Figure 9, and

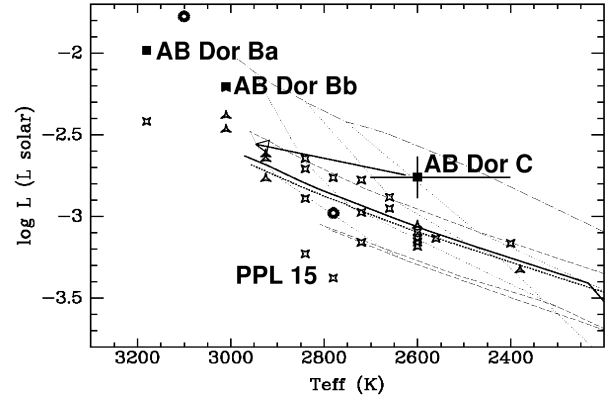


Fig. 9. HR diagram showing low-mass Pleiades objects from Martin et al. 2000 (open stars), other low-mass members of the Pleiades taken from the literature (open triangles), and AB Dor Ba/Bb (filled boxes). Both AB Dor Ba/Bb and PPL 15 A/B are shown both as individual objects and as a single, blended source (rings). The dotted vertical lines are iso-mass contours for the DUSTY models (from left to right, 0.09, 0.07, 0.05, and 0.04 M_\odot), while the more horizontal, dashed lines are the DUSTY isochrones (top to bottom, 10, 50, 100, 120, 500, 1000 Myr). Note that the DUSTY models predict a 70–100 Myr object of 0.09 M_\odot should be ~ 400 K hotter than observed. From the location of AB Dor C on the HR diagram, one would derive a mass of 0.04 M_\odot , a factor of 2 underestimate in mass. As the temperature and luminosities of the Pleiades objects in this plot were determined in the same manner used for AB Dor C, and these Pleiades points mostly fall along the appropriate 120 Myr DUSTY isochrone, we are assured that our temperature scale and bolometric correction are reasonable. With 1σ error bars, there is a $\sim 99\%$ chance that the DUSTY models underestimate the mass of AB Dor C from the HR diagram.

move downward (as AB Dor Ba/Bb and PPL 15 do when deblended), appearing consistent with the Pleiades locus. While this interpretation cannot be currently ruled out (though we estimate the likelihood to be $< 5\%$), we will address this issue in more depth in Close et al. 2005, in prep.

Finally, we note an overall trend for young, low-mass objects where dynamic masses have been measured, as shown in Figure 10. There is a global offset to higher luminosities and temperatures for AB Dor C, USco CTIO 5, and Gl 569 Ba/Bb. These results suggest that further work must be done to bring theoretical evolutionary tracks in line with observations.

Acknowledgements. We thank Gael Chauvin for providing an electronic copy of the spectrum of GSC 8047-0232, and Nadja Gorlova for providing spectra of many young, low-mass objects. We also thank the organizers of the ULMF conference for the chance to present this work.

This publication makes use of data products from the Two micron All Sky Survey, which is a joint project of the University of Massachusetts and the Infrared Processing and Analysis Center/California Institute of Technology, funded by the National Aero-

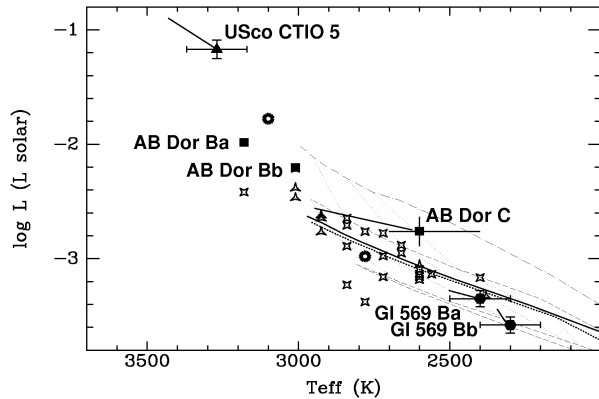


Fig. 10. Again, an HR diagram with the Pleiades and certain other young, low-mass objects, spanning a range of dynamical masses. The points with error bars mark objects with dynamical masses, with the diagonal lines representing the displacement from the measured luminosity and temperature to the values predicted by the DUSTY and Next-Gen models. Upper Sco CTIO 5 (Reiners et al. 2005), AB Dor C, and Gl 569 Ba/Bb (Zapatero Osorio et al. 2004) all show a systematic trend where the measured HR diagram location is cooler and fainter than the models' predictions. Seen another way, the masses predicted by the models are underestimates of the actual masses. In the case of the older (300 Myr) Gl 569 B system, the offset is within the 1σ uncertainties.

nautics and Space Administration and the National Science Foundation.

References

- Allen, P.R., Trilling, D.E., Korner, D.W., Reid, I.N.: 2003 ApJ 595, 1222A.
- Baraffe, I., Chabrier, G., Allard, F., & Hauschildt, P.H.: 1998 A&A 337 403B.
- Burrows, A., Sudarsky, D., & Lunine, J.I.: 2003 ApJ 569, 587B.
- Briggs, K.R. & Pye, J.P.: 2004 MNRAS 353, 673B.
- Chabrier, G., Baraffe, I., Allard, F., & Hauschildt, P.H.: 2000 ApJ 542, 464.
- Chauvin, G., Lagrange, A.M., Lacombe, F., et al.: 2005 A&A 430, 1027C.
- Close, L.M., Lenzen, R., Guirado, J.C., et al.: 2005 Nature 433, 286.
- Cushing, M.C., Rayner, J.T., & Vacca, W.D.: 2005 ApJ 623, 1115C.
- Festin, L.: 1998 MNRAS 298, 34F.
- Gorlova, N.I., Meyer, M.R., Rieke, G.H., & Liebert, J.: 2003 ApJ 593, 1074G.
- Guirado, J.C., Reynolds, J.E., Lestrade, J.-F., et al.: 1997 ApJ 490, 835G.
- Guirado, J.C., et al.: 2005 submitted.
- Lenzen, R., Close, L., Brandner, W., Biller, B., & Hartung, M.: 2004 SPIE 5492, 970L.
- Lenzen, R., Hartung, M., Brandner, W., et al.: 2003 SPIE 4841, 944L.
- Luhman, K.L.: 1999 ApJ 525, 466L.
- Luhman, K.L., Stauffer, J.R. & Mamajek, E.E.: 2005 ApJ 628, 69L.
- Hillenbrand, L.A. & White, R.J.: 2004 ApJ 604, 741H.
- Maiolino, R., Rieke, G.H. & Rieke, M.J.: 1996 AJ 111, 537.
- Marley, M.S., Fortney, J., Hubickyj, O., Saumon, D., et al. 2005 Presentation, 2005 Winter Conference on Astrophysics.

- Marois, C., Macintosh, B., Song, I., Barman, T.: 2005 astro-ph/0502382.
- Martin, E.L.: 2005 private communication.
- Martin, E.L., Brandner, W., Bouvier, et al.: 2000 ApJ 543, 299M.
- Martin, E.L., Rebolo, R. & Zapatero-Osorio, M.R.: 1996 ApJ 469, 706M.
- Mohanty, S., Jayawardhana, R., & Basri, G.: 2004 ApJ 609, 885M.
- Pinfield, D.J., Dobbie, P.D., Jameson, R.F., Steele, I.A., Jones, H.R.A. & Katsiyannis, A.C.: 2003 MNRAS 342, 1241P.
- Reiners, A., Basri, G., & Mohanty, S.: 2005 accepted to ApJ, astro-ph/0506501.
- Terndrup, D.M., Krishnamurthi, A., Pinsonneault, M.H., & Stauffer, J.R.: 1999 AJ 118, 1814T.
- Zapatero Osorio, M. R., Lane, B.F., Pavlenko, Ya., Martin, E.L., Britton, M., & Kulkarni, S.R.: 2004 ApJ 615, 958Z.
- Zuckerman, B., Song, I., & Bessell, M.S.: 2004 ApJ 613L, 65Z.